

# Intracellular pH regulation of CA1 neurons in Na<sup>+</sup>/H<sup>+</sup> isoform 1 mutant mice

Hang Yao,<sup>1</sup> Enbo Ma,<sup>1</sup> Xiang-Qun Gu,<sup>1</sup> and Gabriel G. Haddad<sup>1,2</sup>

<sup>1</sup>Department of Pediatrics, Section of Respiratory Medicine, and

<sup>2</sup>Department of Cellular and Molecular Physiology, Yale University School of Medicine, New Haven, Connecticut 06520, USA

Address correspondence to: Gabriel G. Haddad, Yale University School of Medicine, Department of Pediatrics, Section of Respiratory Medicine, Fitkin Memorial Pavilion, Room 506, 333 Cedar Street, New Haven, Connecticut 06510, USA. Phone: (203) 785-5444; Fax: (203) 785-6337; E-mail: gabriel.haddad@yale.edu.

Received for publication March 11, 1999, and accepted in revised form July 13, 1999.

To understand the role of Na<sup>+</sup>/H<sup>+</sup> exchanger 1 (NHE1) in intracellular pH (pH<sub>i</sub>) regulation and neuronal function, we took advantage of natural knockout mice lacking NHE1, the most ubiquitously and densely expressed NHE isoform in the central nervous system (CNS). CA1 neurons from both wild-type (WT) and NHE1 mutant mice were studied by continuous monitoring of pH<sub>i</sub>, using the fluorescent indicator carboxy-seminaphthorhodafluor-1 (SNARF-1) and confocal microscopy. In the nominal absence of CO<sub>2</sub>/HCO<sub>3</sub><sup>-</sup>, steady-state pH<sub>i</sub> was higher in WT neurons than in mutant neurons. Using the NH<sub>4</sub>Cl prepulse technique, we also show that H<sup>+</sup> flux in WT neurons was much greater than in mutant neurons. The recovery from acid load was blocked in WT neurons, but not in mutant neurons, by removal of Na<sup>+</sup> from the extracellular solution or by using 100 μM 3-(methylsulfonyl-4-piperidino-benzoyl)-guanidine methanesulfonate (HOE 694) in HEPES buffer. Surprisingly, in the presence of CO<sub>2</sub>/HCO<sub>3</sub><sup>-</sup>, the difference in H<sup>+</sup> flux between WT and mutant mice was even more exaggerated, with a difference of more than 250 μM/s between them at pH 6.6. H<sup>+</sup> flux in CO<sub>2</sub>/HCO<sub>3</sub><sup>-</sup> was responsive to diisothiocyanato-stilbene-2,2'-disulfonate (DIDS) in the WT but not in the mutant. We conclude that (a) the absence of NHE1 in the mutant neurons tended to cause lower steady-state pH<sub>i</sub> and, perhaps more importantly, markedly reduced the rate of recovery from an acid load; and (b) this difference in the rate of recovery between mutant and WT neurons was surprisingly larger in the presence, rather than in the absence, of HCO<sub>3</sub><sup>-</sup>, indicating that the presence of NHE1 is essential for the regulation and/or functional expression of both HCO<sub>3</sub><sup>-</sup>-dependent and -independent transporters in neurons. *J. Clin. Invest.* **104**:637–645 (1999).

## Introduction

The regulation of intracellular pH (pH<sub>i</sub>) has been shown to be crucial for many cellular processes (1). In nerve cells, changes in pH<sub>i</sub> can affect neuronal excitability by virtue of their effects on ion channel regulation (2, 3). Furthermore, because neuronal activity can alter pH<sub>i</sub> and neuronal activity can vary enormously from one neuron to another in the central nervous system (CNS), the production of metabolic acids can vary greatly; hence, mechanisms for acid extrusion or acid loading in neurons would be critical for homeostasis. Finally, because of their high metabolic rate, neurons may be susceptible to injury if exposed to wide swings in acid loading, as can happen in excessive activity or during conditions of anoxia or ischemia. Therefore, pH regulation of neurons is likely to be crucial in both physiological and pathophysiological conditions.

Previous work has demonstrated the presence of at least 3 acid extruders in CNS cells, a major one being the electroneutral Na<sup>+</sup>/H<sup>+</sup> exchanger (NHE) (4–12). The function of this NHE is important because its acid-extrusion mechanism is activated mainly at low pH<sub>i</sub> levels, a situation that may lead to cell damage if not rectified (13). Na<sup>+</sup>/H<sup>+</sup> exchange in the CNS of rats takes

place by at least 5 members (NHE1–5) of this gene family. Although there are a number of these exchangers, NHE1 is by far the most ubiquitously expressed and, in most CNS areas, the most densely expressed NHE by at least a fold difference (14, 15). The properties of the NHE in the CNS seem to be similar to those in the heart and kidney, except that, unlike in other tissues, the Na<sup>+</sup>/H<sup>+</sup> exchange in some cell types, including cultured and freshly dissociated hippocampal neurons, is not blocked by amiloride and its derivatives (5, 16).

Because of the multiplicity of the NHEs and the seeming paucity of pharmacological tools to dissect out the role of each of these exchangers, especially in neurons, we took advantage of a naturally occurring mouse mutant, totally lacking the NHE1 isoform, to study the effect of this mutation on pH<sub>i</sub> homeostasis. We chose to examine the effect of this mutation in hippocampal neurons because these have been well studied by our group and others (17, 18). We acutely isolated hippocampal CA1 neurons from NHE1 mutant and wild-type (WT) mice to conduct these experiments. We hypothesized that mutant CA1 neurons, which lacked the NHE1, would upregulate other mechanisms, such as the HCO<sub>3</sub><sup>-</sup>-dependent mechanisms, to compensate for the deficiency in NHE1.

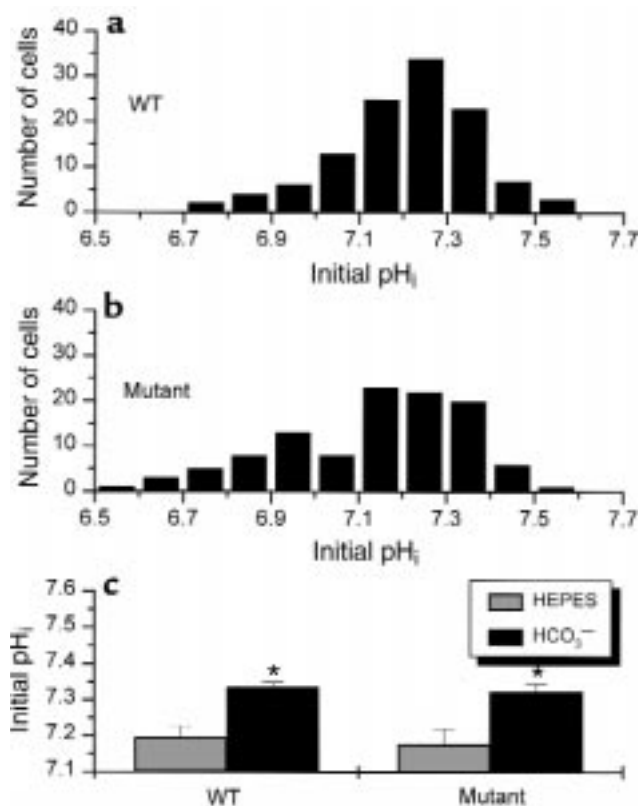


**Figure 1** Distribution of steady-state pH<sub>i</sub> in CA1 neurons isolated from WT and NHE1 mutant mice. (a) Steady-state pH<sub>i</sub> of CA1 neurons ( $n = 117$ ) isolated from 57 WT mice is illustrated as a frequency histogram with a bin width of 0.1 pH unit. Mean  $\pm$  SD of steady-state pH<sub>i</sub> for WT is  $7.25 \pm 0.15$ . (b) The distribution of steady-state pH<sub>i</sub> of CA1 neurons ( $n = 110$ ) isolated from 61 NHE1 mutant mice is shifted to the left. Mean  $\pm$  SD is  $7.17 \pm 0.20$  (NHE1 vs. WT;  $P < 0.05$ ). (c) In HEPES buffer, the steady-state pH<sub>i</sub> is significantly lower than in the CO<sub>2</sub>/HCO<sub>3</sub><sup>-</sup>-buffered solution in both WT and mutant mice ( $*P < 0.05$ ).

## Methods

**Cell preparation.** B6.SJL, +/Swe (slow-wave epilepsy) mice were obtained from The Jackson Laboratory (Bar Harbor, Maine, USA) (19). These heterozygous mice (+/Swe) were mated in our institution, and the resulting homozygous NHE1 mutant (25%) and WT (25%) F1 mice progeny were used. Although homozygous mutant mice had a clear phenotype consisting of locomotor ataxia in the hindlimbs and a slow, wide-based gait and coarse truncal instability starting at about 2–3 weeks of age, a PCR-based test was always performed to confirm the genotype (see below). Mice 21–30 days old were used, and their hippocampi were removed and sliced into 7–10 transverse sections 400  $\mu$ m thick. The slices were immediately transferred to a container with 25 mL of fresh, oxygenated, and slightly stirred HEPES buffer at room temperature. After 30 minutes of exposure to trypsin (0.08%) and 20 minutes of protease (0.05%) digestion, the slices were washed several times with HEPES buffer and left in oxygenated solution. The CA1 region was then dissected out and triturated

in a small volume (0.25 mL) of HEPES buffer. These studies have been approved by the Yale Animal Care and Use Committee.

**Solutions.** The HEPES-buffered solution contained 125 mM NaCl, 3 mM KCl, 1.2 mM CaCl<sub>2</sub>, 1.2 mM MgSO<sub>4</sub>, 1.25 mM NaH<sub>2</sub>PO<sub>4</sub>, 30 mM HEPES, and 10 mM glucose. This solution was titrated to pH 7.38 at 35°C with NaOH. In the NH<sub>4</sub><sup>+</sup>/NH<sub>3</sub> solution, 20 mM NaCl was replaced with the same concentration of NH<sub>4</sub>Cl. For the CO<sub>2</sub>/HCO<sub>3</sub><sup>-</sup> solution, HEPES was replaced by 22 mM NaHCO<sub>3</sub> and bubbled with 5% CO<sub>2</sub>. Nigericin calibration solution contained 105 mM KCl, 50 mM *N*-methyl-D-glucammonium (NMDG), 5 mM MgSO<sub>4</sub>, 10 mM glucose, and 30 mM HEPES. TNE buffer contained 10 mM Tris (pH 7.5), 400 mM NaCl, 100 mM EDTA, 0.6% SDS. TE buffer contained 10 mM Tris (pH 8.0) and 10 mM EDTA. Carboxy-seminaphthorhodafleur-1 (SNARF-1) was obtained from Molecular Probes Inc. (Eugene, Oregon, USA). Nigericin, amiloride, diisothiocyanato-stilbene-2,2'-disulfonate (DIDS), and ethylisopropyl-amiloride (EIPA) were purchased from Sigma Chemical Co. (St. Louis, Missouri, USA). The 3-(methylsulfonyl-4-piperidino-benzoyl)-guanidine methanesulfonate (HOE 694) was a gift from Hans-J. Lang (HMR/Hoechst Marion Roussel Chemical Research, Frankfurt, Germany).

**pH<sub>i</sub> measurements.** Just before each experiment, neurons were plated and fixed on a coverslip that was pre-coated with Cell-Tak (Collaborative Research Inc., Bedford, Massachusetts, USA). The coverslip was placed on the stage of a Zeiss inverted microscope (Carl Zeiss, Inc., Thornwood, New York, USA) attached to a Bio-Rad MRC 600 laser confocal scanning unit (Bio-Rad, Hercules, California, USA). The cells were loaded with 10  $\mu$ M of the acetoxymethylester form of SNARF-1 (SNARF-1-AM, prepared in dimethyl sulfoxide) for about 20 minutes. After loading the dye, a single pyramid-shaped CA1 neuron was selected for pH<sub>i</sub> measurements. The intracellular dye was excited at the 514-nm wavelength, and the emission was detected by 2 photomultiplier tubes at 2 wavelengths (587 and 640 nm) for ratiometric analysis. Each sample data point was acquired every 8 seconds for both wavelengths, and the image of a single neuron was stored on a hard disk, frame by frame, and analyzed off-line (software supplied by Bio-Rad Laboratories Inc., as well as developed in our laboratory). Ratios were obtained from the 2 fluorescence-emission intensities, and the values were converted to pH<sub>i</sub> using the following equation:

### (Equation 1)

$$\text{pH} = \log \left\{ \frac{(R/R_{\text{pH}=7}) - R_{\text{min}}}{R_{\text{max}} - (R/R_{\text{pH}=7})} + \text{pK} \right\}$$

where  $R$  is the ratio,  $R_{\text{min}}$  is the minimum ratio,  $R_{\text{max}}$  is the maximum ratio,  $R_{\text{pH}=7}$  is the ratio at pH 7.0, and  $\text{pK}$  is  $-\log$  of the dissociation constant. Values of  $R_{\text{min}}$  (0.18),  $R_{\text{max}}$  (1.34), and  $\text{pK}$  (7.39) were calculated using the calibration described previously (16, 20, 21). Cali-

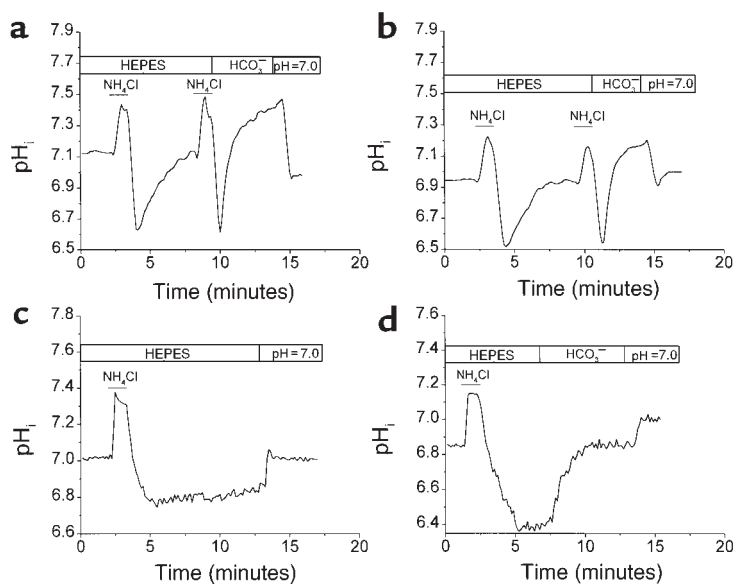


**Figure 2**

Examination of recovery from acid loading in both WT and NHE1 mutant CA1 neurons in the presence and absence of  $\text{CO}_2/\text{HCO}_3^-$ . (a)  $\text{CO}_2/\text{HCO}_3^-$  enhances the recovery from an acid load in a WT CA1 neuron. A single CA1 neuron was acid-loaded twice with HEPES solution containing 20 mM  $\text{NH}_4\text{Cl}$ . The cell was allowed to recover first in the absence, and then in the presence, of  $\text{CO}_2/\text{HCO}_3^-$ . This WT cell promptly recovered from the acid load in both solutions, and with a faster recovery rate when the  $\text{CO}_2/\text{HCO}_3^-$  was present. (b) CA1 neurons isolated from NHE1 mutant mice exhibit different patterns of  $\text{pH}_i$  recovery from acid load. Although recovery from acid loads was present in this mutant neuron, the rates in the presence or absence of  $\text{CO}_2/\text{HCO}_3^-$  were lower than in the WT. (c) Another mutant neuron was studied. In this experiment, the mutant neuron does not recover in HEPES buffer, even 10 minutes after acid loading. (d) With  $\text{CO}_2/\text{HCO}_3^-$ ,  $\text{pH}_i$  of this kind of mutant cell recovers from acid loading to the starting level, albeit at a much reduced rate. At the end of each experiment, the cell was exposed to nigericin calibration solution ( $\text{pH} = 7.0$ ) for calibration.

bration experiments were done in both WT and NHE1 mutant neurons, and no significant difference was found between them. Each  $d\text{pH}_i/dt$  value was calculated by first fitting the data to the Boltzman equation, and then averaging  $d\text{pH}_i/dt$  over 0.2 pH units from each function obtained. The intrinsic intracellular buffering power ( $\beta_i$ ) was obtained by decreasing the external concentration of the weak base  $\text{NH}_3$ , measuring the corresponding  $\text{pH}_i$  in a stepwise manner, and then calculating it as described by Boyarsky et al. (21) and Bevensee et al. (17). The calculation of buffering power due to  $\text{CO}_2/\text{HCO}_3^-$  ( $\beta_{\text{HCO}_3^-}$ ) was based on the theoretical analysis of Roos and Boron (22). The total buffering power of the neuron was computed by  $\beta_T = \beta_i + \beta_{\text{HCO}_3^-}$ .

We selected the cells that did not show grainy and flat surfaces, because these cells could have been injured. Furthermore, during off-line analysis, we used neurons that did not show a dye loss of more than 5% per minute (23).

**Genotyping of NHE1 mutant mice.** Although the phenotype of the mutant mice was easily detected by their behavior, we did not rely on it solely. We performed genotyping on all presumed mutant mice to confirm the phenotypic differences. Genomic DNA was obtained from mice tails and used for PCR amplification with the primers:

5'-TCGCCTCAGGAGTAGTGATGCG-3' (sense) and 5'-CGTCTTGTGCAGGGCATGA-3' (antisense), corresponding to bp's 1397-1418 and 1800-1819, respectively, of mouse NHE1 cDNA sequence (GenBank accession no. U51112). The amplification program was set at 94°C for 1.5 minutes, 60°C for 1 minute, and 72°C for 1.5 minutes, for 30 cycles. DNA was subjected to the endonuclease *Spe1* in order to differentiate between WT and homozygous mutant genotype. The basis for the difference in band pattern was a single nucleotide difference (change from A in the WT to a T in the mutant, resulting in a TAG and a stop codon).

This transforms the surrounding sequence from CAA-CAAGTTCC to CAACTAGTTCC. *Spe1*, which cuts between A and C in the sequence ACTAG, cleaves the mutant molecule (2 bands) but not the WT (1 band).

**Statistics.** Data are presented as mean  $\pm$  SD. Levels of significance were assessed using paired and unpaired forms of the Student's *t* test. Differences in means were considered significant when the *P* value was less than 0.05. Rate constants of  $\text{pH}_i$  recovery from intracellular acid loads were determined by fitting the data to a Boltzman function using a least squares method.

## Results

**Resting  $\text{pH}_i$  in CA1 neurons.** We studied steady-state  $\text{pH}_i$  of CA1 neurons in either HEPES or  $\text{CO}_2/\text{HCO}_3^-$  solution. Figure 1 illustrates the frequency distribution of steady-state  $\text{pH}_i$  values for CA1 neurons isolated from both WT and NHE1 mutant mice in HEPES solution. As we have described previously in rat neurons (17), CA1 neurons from mice also have a broad range of initial  $\text{pH}_i$ . The steady-state  $\text{pH}_i$  for WT neurons ranged from 6.75 to 7.55, and that for NHE1 mutant mice neurons ranged from 6.55 to 7.55. Mean steady-state  $\text{pH}_i$  for WT was  $7.25 \pm 0.15$  ( $n = 117$ ), significantly higher than that for the NHE1 mutant mice, which was  $7.17 \pm 0.20$  ( $P < 0.05$ ;  $n = 110$ ). Figure 1, a and b show that mutant neurons were more likely to have lower initial  $\text{pH}_i$  values than WT neurons. For example, 27% of neurons in mutant mice had a  $\text{pH}_i$  less than 7.0, whereas the same was true for only 11% of WT neurons. The median steady-state  $\text{pH}_i$  of WT neurons was exactly the same as their mean, but the median of mutant neurons was higher than the mean, indicating that distribution was skewed to the left in the mutant neurons.

Switching from HEPES to a  $\text{CO}_2/\text{HCO}_3^-$ -buffered solution in a subset of WT and mutant neurons caused steady-state  $\text{pH}_i$  to increase by a mean difference of  $0.14 \pm 0.02$  ( $P < 0.001$ , paired *t* test;  $n = 19$ ) in WT mice, and by



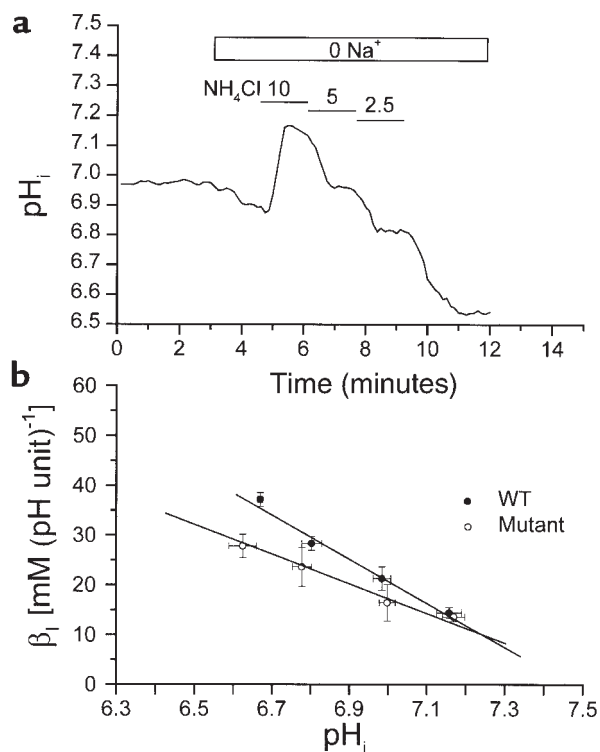


**Figure 3** Measurement of intrinsic intracellular buffering power. (a) Experiment on a WT CA1 neuron. The CA1 neuron was first bathed with HEPES buffer containing  $\text{Na}^+$ , and then switched to one without  $\text{Na}^+$  to block the  $\text{Na}^+$ -dependent ion exchange. The cell was subsequently exposed to 10 mM, 5 mM, 2.5 mM, and 0 mM  $\text{NH}_3/\text{NH}_4^+$ , respectively. The cell responded by gradually reducing  $\text{pH}_i$ . (b) Relation of intrinsic intracellular buffering power ( $\beta_i$ ) as a function of  $\text{pH}_i$ . Data are summarized from 7 experiments on WT mice and 10 experiments on NHE1 mutant mice. Each  $\beta_i$  was calculated within  $\text{pH}_i$  intervals of 0.2.

$0.15 \pm 0.02$  ( $P < 0.001$ , paired  $t$  test;  $n = 29$ ) in mutant mice (Figure 1c). Thus,  $\text{CO}_2/\text{HCO}_3^-$  produced an increase in steady-state  $\text{pH}_i$  in both WT and mutant neurons, suggesting that  $\text{HCO}_3^-$ -dependent acid-extrusion mechanisms overwhelm any acid-loading mechanisms that depend on  $\text{HCO}_3^-$  in the steady-state  $\text{pH}_i$  regulation.

**pH<sub>i</sub> recovery from an acid load.** Previous work has already shown that in rat CA1 neurons, the recovery of  $\text{pH}_i$  from an acid load involves both  $\text{HCO}_3^-$ -dependent and -independent transport mechanisms (16). To examine both types of mechanisms in mice CA1 neurons, we acid-loaded the cell twice using the  $\text{NH}_4^+$  prepulse technique (24), and then allowed each cell to recover in either HEPES or  $\text{CO}_2/\text{HCO}_3^-$  solution. Figure 2 shows the response of both WT and NHE1 mutant neurons after acid loading. Figure 2a shows the results of a typical experiment on a WT CA1 neuron, first in HEPES and then in  $\text{CO}_2/\text{HCO}_3^-$  solution. This WT cell promptly recovered from the acid load in HEPES, with the  $\text{pH}_i$  increasing to approximately the starting level. In the  $\text{CO}_2/\text{HCO}_3^-$ -buffered solution, recovery from a similar acid load was faster, and  $\text{pH}_i$  returned to a baseline that was higher than with HEPES, an expected result. In Fig-

ure 2, b and c, however, we show that mutant mice CA1 neurons had a different response to acid loading than did WT neurons. First, unlike the homogeneous response to acid loading in WT cells, cells from the mutant mice seemed to fall in either of 2 groups of cells that had 2 different response patterns. Second, one pattern was similar to that of the WT cells qualitatively, but not quantitatively, in both HEPES and  $\text{CO}_2/\text{HCO}_3^-$  solutions; the other response pattern was qualitatively and strikingly different than that of the WT cells. Figure 2b is an example of the first pattern group (group 1, G1), which represented the majority of mutant cells (approximately 85% of mutant CA1 neurons). In the second pattern group (group 2, G2), which represented the rest of the cells, neurons could not recover to the initial  $\text{pH}_i$  level (Figure 2c) in HEPES buffer. When the solution was switched to  $\text{CO}_2/\text{HCO}_3^-$ , the  $\text{pH}_i$  of the cell recovered, albeit at a slower rate (Figure 2d).

**Measurement of intrinsic intracellular buffering power of CA1 neurons in mice.** We measured intrinsic intracellular buffering power ( $\beta_i$ ) so that the net efflux of  $\text{H}^+$  could be computed from the rates of  $\text{pH}_i$  recovery in both HEPES ( $\beta_i$ ) and bicarbonate ( $\beta_T = \beta_i + \beta_{\text{HCO}_3^-}$ ) solutions. Figure 3a shows an experiment in a WT CA1 neuron in which the intrinsic buffering power was measured. Figure 3b shows the  $\text{pH}_i$  dependence of intrinsic buffering power in WT and NHE1 mutant mice. The best-fit line to the data had a slope of  $-44.28 \pm 4.05$  mM/ $\text{pH}^2$  and a y-intercept of  $330.78 \pm 28.20$  mM/ $\text{pH}$  in WT neurons, and a smaller slope of  $-29.74 \pm 9.62$  mM/ $\text{pH}^2$  and y-intercept of  $225.48 \pm 66.35$  mM/ $\text{pH}$  in NHE1 mutant mice.

**Differences in H<sup>+</sup> flux between WT and NHE1 mutant neurons.** In both HEPES and  $\text{CO}_2/\text{HCO}_3^-$  solutions, both WT and mutant neurons extrude  $\text{H}^+$  in a  $\text{pH}_i$ -dependent manner. Figure 4a shows that mutant G1, and especially WT neurons, exhibit a clear  $\text{pH}_i$ -dependent behavior of  $\text{H}^+$  flux in HEPES buffer. At the higher  $\text{pH}_i$  range, both mutant G1 and WT CA1 neurons had significantly lower  $\text{H}^+$  extrusion rates than at the lower  $\text{pH}_i$  range. G1 neurons, however, had a smaller flux than WT at these low  $\text{pH}_i$  levels. Compare, for example, the rates at  $\text{pH}_i$  6.5–6.7 and 6.7–6.9:  $93.1 \pm 25.0$   $\mu\text{M}/\text{s}$  and  $70.2 \pm 15.8$   $\mu\text{M}/\text{s}$  for mutants, and  $191.8 \pm 8.2$   $\mu\text{M}/\text{s}$  and  $137.9 \pm 28.5$   $\mu\text{M}/\text{s}$  for WT ( $P = 0.018$  and  $P = 0.038$ , respectively) (Figure 4a), a difference of about 60–100  $\mu\text{M}/\text{s}$ . G2 neurons had very little recovery from an acid load at the lower  $\text{pH}_i$  range (6.5–6.9); their  $\text{H}^+$  flux, therefore, was almost nil.

Figure 4b shows the  $\text{H}^+$  flux rate of WT and G1 neurons in the presence of  $\text{CO}_2/\text{HCO}_3^-$ .  $\text{H}^+$  flux in both WT and G1 mutant neurons in  $\text{CO}_2/\text{HCO}_3^-$  was higher than in HEPES (Figure 4a), especially at the lower  $\text{pH}_i$  range. The flux in the G1 mutant neurons was much smaller than in the WT neurons in the presence of  $\text{CO}_2/\text{HCO}_3^-$ . For example, at  $\text{pH}_i$  6.5–6.7 and 6.7–6.9, the flux rate was  $318.8 \pm 50.7$   $\mu\text{M}/\text{s}$  and  $245.3 \pm 36.9$   $\mu\text{M}/\text{s}$  in the mutant G1 neurons, compared with  $561.6 \pm 110.7$   $\mu\text{M}/\text{s}$  and  $438.5 \pm 70.2$   $\mu\text{M}/\text{s}$  in the WT ( $P = 0.047$  and  $P = 0.028$ , respectively). In Figure 4c, we com-

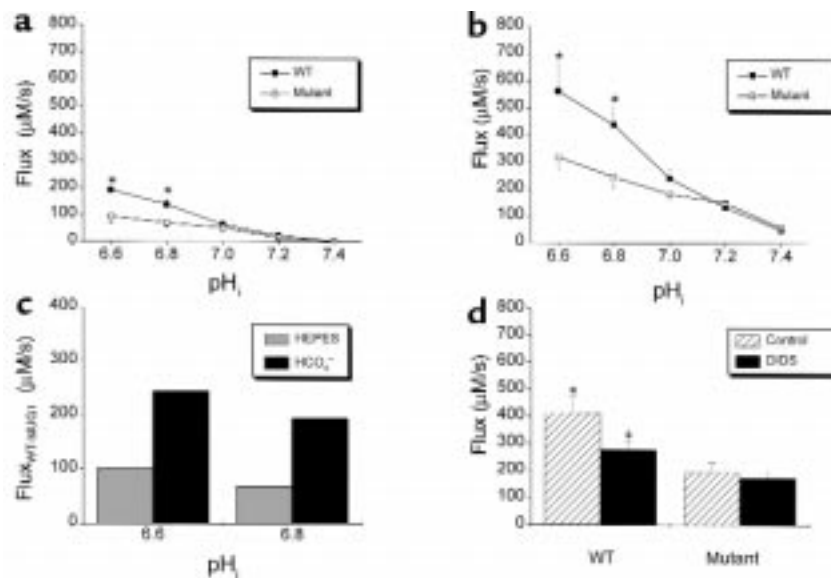


**Figure 4**

Differences in  $\text{H}^+$  flux between WT and NHE1 mutant neurons, and response to DIDS. (a) In the absence of  $\text{CO}_2/\text{HCO}_3^-$ ,  $\text{H}^+$  flux rate in both WT and mutant (G1) neurons increased with decreasing  $\text{pH}_i$ . At a  $\text{pH}_i$  range of 6.5–6.9, mutant neurons ( $n = 18$ ) exhibited a smaller  $\text{H}^+$  flux than WT neurons ( $n = 15$ ).  $*P < 0.05$ . (b) In the presence of  $\text{CO}_2/\text{HCO}_3^-$ , both WT and mutant G1 neurons showed higher  $\text{H}^+$  flux rate. Interestingly, however, G1 neurons ( $\text{pH}_i$  6.5–6.9;  $n = 24$ ) showed a much smaller  $\text{H}^+$  flux than WT neurons ( $n = 17$ ).  $*P < 0.05$ . (c) Difference in flux rate between WT and mutant neurons in the presence and absence of  $\text{CO}_2/\text{HCO}_3^-$ . Note the much larger difference in  $\text{HCO}_3^-$  solutions at  $\text{pH}$  6.5–6.7 and 6.7–6.9. (d) Summary of DIDS sensitivity of both WT and NHE1 mutant neurons. Control experiments refer to measurements of  $\text{H}^+$  flux before the application of DIDS. DIDS (400  $\mu\text{M}$ ) was then applied in a subset of neurons from both WT ( $n = 7$ ) and NHE1 mutant G1 neurons ( $n = 8$ ). A significant DIDS-induced reduction of  $\text{H}^+$  flux is observed in WT neurons ( $*P < 0.05$  control vs. DIDS) but not in the mutant, indicating that the mutant lacks a DIDS-sensitive component of  $\text{H}^+$  flux. There was also a statistically significant difference between  $\text{H}^+$  flux during DIDS in the WT neurons and that in mutant neurons ( $*P < 0.05$  WT vs. mutant G1 neurons), possibly indicating that a component of the DIDS-insensitive portion of  $\text{H}^+$  flux is also absent in the mutant neurons.

pared the  $\text{H}^+$  flux differences between WT and G1 mutant neurons. At  $\text{pH}$  ranges of 6.5–6.7 and 6.7–6.9, the  $\text{H}^+$  flux rate difference between G1 and WT mutant cells was markedly smaller in HEPES solutions than in  $\text{CO}_2/\text{HCO}_3^-$  solutions, and the difference amounted to about 200–250  $\mu\text{M/s}$ . This result was surprising. To understand the basis for this larger difference in  $\text{H}^+$  flux in mutant mice, we used 400  $\mu\text{M}$  DIDS in the  $\text{CO}_2/\text{HCO}_3^-$ -buffered solution to block  $\text{CO}_2/\text{HCO}_3^-$ -dependent acid extrusion. Within the  $\text{pH}_i$  range of 6.5–6.9, the reduction in  $\text{H}^+$  flux by DIDS was small and insignificant ( $n = 8$ ) in mutant mice, but 32.6% (from  $412.6 \pm 58.6 \mu\text{M/s}$  to  $277.8 \pm 30.5 \mu\text{M/s}$ ;  $P < 0.05$ ,  $n = 7$ ) in WT mice (Figure 4d). Furthermore, there was a significantly smaller  $\text{H}^+$  flux in the mutant mice than in the WT after the application of DIDS. This indicated that (a) there are 2 components of  $\text{HCO}_3^-$ -dependent mechanisms in the WT, one sensitive and the other insensitive to DIDS; and (b)  $\text{HCO}_3^-$ -dependent mechanisms in the mutant neurons are attenuated, and the DIDS-sensitive portion is almost totally eliminated.

*Effect of  $\text{Na}^+$  removal and NHE blockers on  $\text{pH}_i$  regulation in HEPES.* Figure 5a shows the effect of external  $\text{Na}^+$  removal (replaced by NMDG $^+$ ) on steady-state  $\text{pH}_i$  in a WT neuron. The response of this cell was that of a prompt acidification upon  $\text{Na}^+$  withdrawal from HEPES buffer and a maintenance of the  $\text{pH}_i$  at low levels. When

the solution was switched back to the HEPES buffer with  $\text{Na}^+$ , the  $\text{pH}$  of this cell recovered toward baseline and had an overshoot. In the WT neurons,  $\text{pH}_i$  changed by  $0.39 \pm 0.03$  ( $n = 15$ ) with  $\text{Na}^+$  removal, whereas in mutant neurons, the difference was  $0.33 \pm 0.03$  ( $n = 16$ ), a smaller change in  $\text{pH}_i$  in the mutants. We also examined the effect of  $\text{Na}^+$  removal on the acid extrusion in both WT and mutant neurons. Figure 5b shows an example of these experiments in WT neurons. After the first acidification, the cell was allowed to recover in standard HEPES buffer; after the second acidification, the recovery was challenged by withdrawing  $\text{Na}^+$  from the external solution. In WT neurons ( $n = 11$ ), at the  $\text{pH}_i$  range of 6.5–6.9,  $\text{Na}^+$  removal caused  $\text{H}^+$  flux to be reduced from  $104.8 \pm 10.6 \mu\text{M/s}$  to  $41.3 \pm 9.7 \mu\text{M/s}$  ( $P < 0.05$ ), a 60.5% reduction. In mutant neurons ( $n = 14$ ), however, flux was reduced slightly from  $45.3 \pm 3.5 \mu\text{M/s}$  to  $38.4 \pm 6.9 \mu\text{M/s}$  ( $P > 0.10$ ) in the same  $\text{pH}_i$  range (Figure 5c). Thus, in the absence of  $\text{CO}_2/\text{HCO}_3^-$ , CA1 neurons from WT mice extrude  $\text{H}^+$  by  $\text{Na}^+$ -dependent mechanisms, most likely by  $\text{Na}^+/\text{H}^+$  exchange. The acid-extrusion process seems to be much less  $\text{Na}^+$ -dependent in the NHE1 mutant mice than in WT mice.

To determine if NHE plays an important role in  $\text{pH}_i$  regulation in CA1 neurons, we also examined the effects of NHE blockers on  $\text{pH}_i$  recovery from acid loading in HEPES solution. However, the conventional blockers of

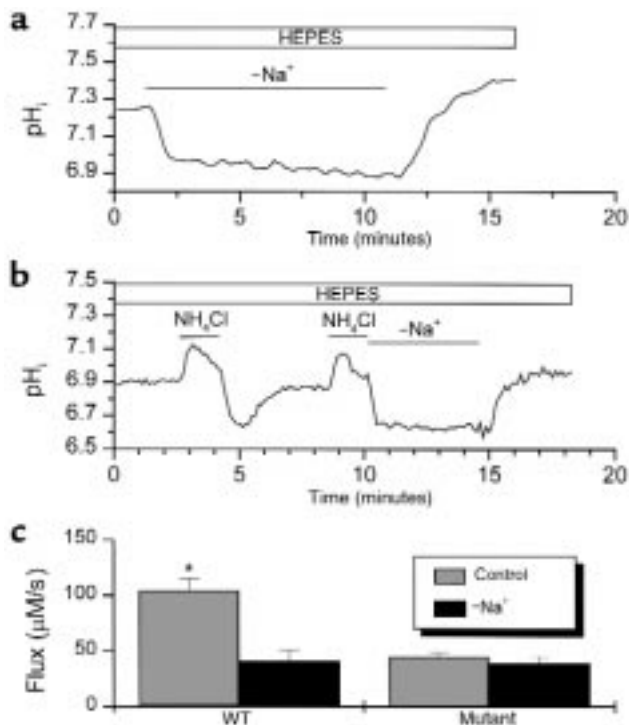


**Figure 5** Na<sup>+</sup> dependency of pH<sub>i</sub> regulation in WT and mutant CA1 neurons. (a) The effect of Na<sup>+</sup> removal on the steady-state pH<sub>i</sub> regulation in a WT neuron. Each neuron was studied in HEPES buffer and in a non-Na<sup>+</sup>-containing HEPES buffer. Steady-state pH<sub>i</sub> fell and remained at a low level until the external solution was switched back to standard, Na<sup>+</sup>-containing HEPES buffer. (b) The effect of Na<sup>+</sup> removal on the recovery from acid load in a WT neuron. The neuron was acid-loaded twice in this experiment. After the first acidification, the neuron was allowed to recover in a standard Na<sup>+</sup>-containing HEPES buffer. The pH<sub>i</sub> of the cell recovered to baseline. The recovery, however, was blocked when the neuron was exposed to a non-Na<sup>+</sup>-containing HEPES buffer after the second acidification. (c) Summary of 11 experiments in WT neurons and 14 experiments in mutant neurons. In non-Na<sup>+</sup>-containing HEPES solution, a significant reduction (at pH range of 6.5–6.9) in H<sup>+</sup> flux was observed in WT neurons but not in mutant neurons. \**P* < 0.05.

NHE, such as amiloride (0.25 mM, 0.5 mM, and 1 mM) and amiloride analogues (EIPA, 50 μM and 200 μM), did not induce any change in acid extrusion (data not shown). These results were similar to those we obtained in rat CA1 neurons (17). On the other hand, HOE 694 (100 μM), a potent NHE1 inhibitor in non-neuronal cell types (25–27), substantially inhibited acid extrusion in WT neurons (Figure 6a). At a pH<sub>i</sub> range of 6.5–6.9, HOE 694 reduced the H<sup>+</sup> flux in WT neurons from 98.5 ± 16.3 μM/s to 48.8 ± 7.5 μM/s (*P* < 0.05; *n* = 4), a 50.4% reduction. However, this inhibition did not occur in mutant neurons, because H<sup>+</sup> flux in these neurons was 48.3 ± 13.1 μM/s before HOE 694 application and 46.2 ± 6.3 μM/s (*n* = 4) after its application (Figure 6b).

## Discussion

**Overview.** Locomotor ataxia, a wide-based gait, and coarse truncal instability during movement constitute

the apparent phenotype in NHE1 mutant mice. These mice also demonstrate seizures, such as absence-type or slow-wave epilepsy (19). These observations would indicate that the NHE1 mutation and its pathophysiological consequences lead to pathology in several CNS areas, including deep cerebellar nuclei, the cortex, and the hippocampus. In addition, because the neurological signs in these mice are relatively not severe, it is reasonable to assume that membrane proteins, such as NHE isoforms other than NHE1 and CO<sub>2</sub>/HCO<sub>3</sub><sup>-</sup>-dependent transporters, could have been activated or overexpressed in order to compensate for the lack of NHE1 function. Because the phenotype in these mutant mice is completely normal before the age of 2–3 weeks, we have investigated pH<sub>i</sub> regulation in neurons of mice over 3 weeks old.

We studied CA1 neurons in WT and NHE1 mutant mice for 4 reasons. First, we have recently demonstrated that NHE1 is normally highly expressed in the CA1 layer (14). Second, there is generally more homogeneity in cell types in the CA1 area than in other regions, such as the cortex; this was desirable, because we wished to simplify our task. Third, we and others have had a long-standing interest in the hippocampal CA1–3 cells, because these cells are rather sensitive to hypoxic cell injury. Fourth, some of the neurological findings in these mice could be attributed to abnormal hippocampal function (19), and, therefore, the likelihood of detecting consequential effects of NHE1 mutation on cell function is high.

The role of this NHE1 mutation and the lack of NHE1 protein was tested by examining pH<sub>i</sub> in both resting conditions and after stress, e.g., acid loading. In this work, we have made several important observations in CA1 neurons. First, although there was a wide distribution in steady-state pH<sub>i</sub> in both WT and mutant mice, there was a shift to a more acidic pH<sub>i</sub> in the mutant neurons. Second, pH<sub>i</sub> recovery and H<sup>+</sup> flux in response to an acid load was abnormally low in mutant cells, but this was much more attenuated in one group of mutant cells (G2) than in another (G1). Third, surprisingly, the H<sup>+</sup> flux rate in the acid-loaded mutant neurons (G1) was not only abnormal in the nominal absence of HCO<sub>3</sub><sup>-</sup>, but especially in the presence of HCO<sub>3</sub><sup>-</sup> solutions.

**Effect of lack of NHE1 on the regulation of steady-state pH<sub>i</sub>.** In this study, the absence of NHE1 was detected when we compared steady-state pH<sub>i</sub> regulation in the presence and absence of extracellular Na<sup>+</sup> (Na<sup>+</sup><sub>o</sub>). In NHE1 mutant neurons, mean steady-state pH<sub>i</sub> was lower than in the WT neurons. Furthermore, acute withdrawal of Na<sup>+</sup><sub>o</sub> elicited acidification in both WT and mutant neurons, but there was a tendency for a larger reduction in pH<sub>i</sub> in WT neurons, suggesting that the WT neurons rely more on this mechanism than mutant neurons, even in the steady state. It is important to mention here that both WT and NHE1 mutant mice neurons had a wide pH<sub>i</sub> distribution. This wide distribution in CA1 neurons is similar to the pH<sub>i</sub> distribution we described



previously in rat neurons and astrocytes (7, 17). Clearly, a number of mechanisms besides NHE could be contributing to this wide  $pH_i$  distribution. We have argued previously that these neurons may possess different “set points” for acid-base balance, depending on the particular physiological role they play. Because of the lower steady-state  $pH_i$  in mutant neurons, and the wide range in steady-state  $pH_i$  among the cells studied, we raise the question as to whether the cells studied, WT or null, are viable and uninjured. We believe that the mutant and WT neurons were healthy for at least 5 reasons. First, the dissociation procedure has been well established in our laboratory for several years; we have studied such neurons and shown that they have properties of neurons in slices that have not undergone trituration and enzymatic digestion (17). Second, morphological criteria have also been well established; no cells with grainy and flat surface with loss of 3-dimensionality and apparent nucleoli were chosen. Third, we used a dye-loss criterion (less than 5% per minute) (23) to determine cell integrity for both WT and null neurons, and we eliminated any cell that had a higher rate of dye loss for both WT and null neurons. Fourth, if membrane injury and damage had occurred, it would be reasonable to expect a  $pH_i$  that is close to  $pH_o$ , and this contrasts with the lower  $pH_i$  shift that we obtained in the null neurons. Finally, in parallel electrophysiological experiments in our laboratory, using exactly the same techniques of trituration (and often sharing dissociated cells from the same dish), we have found that the membrane potential in the null neurons is very similar to that in the WT neurons in HEPES buffer.

*Reduction of acid extrusion in mutant neurons in the absence of  $HCO_3^-$ .* Much more striking than steady-state  $pH_i$  regulation, however, is the rate at which mutant neurons recover from acid loading. Our observation that the majority of mutant neurons (G1) have a much lower recovery rate than WT neurons after an acid load in the nominal absence of  $HCO_3^-$  leads us to believe that, if other factors are equal, the  $H^+$  flux across the neuronal membrane is smaller in the mutant neurons. However, for reasons that are not clear to us presently, the buffering power in these mutant cells (G1) is also lower than that in WT cells. Hence, this would render  $H^+$  flux even smaller in the G1 mutant neurons, and the lower rate of recovery of  $pH_i$  to an acid load in these mutant neurons is on the basis of an altered neuronal plasma membrane-delimited property. In the nominal absence of  $HCO_3^-$ , this would seem to indicate that the NHE1 null mutation has a major effect on the ability of these neurons to recover from an acid load. The notion that NHE1, and not the other NHE isoforms, has a major role in this recovery is supported further by 2 other observations in this work: (a) the  $Na^+$ -dependent  $H^+$  flux after acid loading is almost nonexistent in the mutant (G1) neurons, unlike in the WT neurons; and (b) HOE 694 has a major effect on the WT  $H^+$  flux but not on the mutant flux. This last result is not unexpected, because these mutant mice

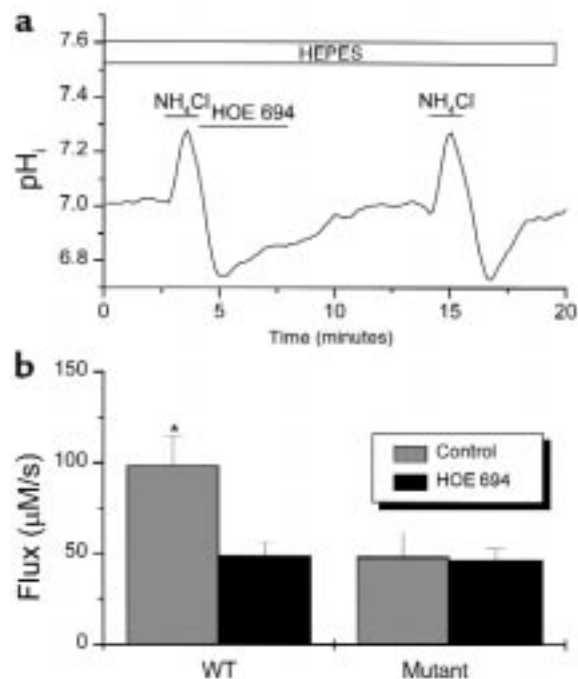


**Figure 6**  
The effect of HOE 694 on the recovery of WT and mutant CA1 neurons from acid load. (a) In an  $NH_4Cl$  prepulse experiment on a WT neuron, 100  $\mu M$  HOE 694 was applied after the first acidification. This graph shows an apparently smaller slope during the application of HOE 694 in the first recovery than in the second one. (b) Summary of the double acid-loading experiments on WT ( $n = 4$ ) and mutant neurons ( $n = 4$ ). Paired comparison analysis showed that 100  $\mu M$  HOE 694 can significantly reduce the  $H^+$  flux rate in WT neurons but not in NHE1 mutant neurons. \* $P < 0.05$ .

do not express any NHE1 protein (unpublished data from our laboratory; ref. 19), and this protein is the major NHE in the CNS. Indeed, we have shown previously, at least at the mRNA level, that the main acid extruder in the CNS in the absence of  $HCO_3^-$  is NHE1. In the CA1, where we obtained these neurons, NHE3 is virtually absent and NHE2 is extremely low in quantity. NHE4 is present in CA1 neurons, but at an order of magnitude lower than NHE1 (14). This analysis of  $H^+$  flux implies also that there has been little, if any, compensatory upregulation of other mechanisms, including NHEs other than NHE1 protein.

Another question should be raised: If mutant G1 neurons can still recover from an acid load (Figure 5c), albeit at a much slower rate, what mechanisms are responsible for this recovery in the absence of both extracellular  $Na^+$  and  $HCO_3^-$ ? In the absence of an upregulation in NHE2, NHE3, and NHE4 isoforms, we postulate that proton pumps or other, potentially novel, acid extruders would be possibilities. Although we thought that the NHE mechanism is the major acid extruder in the nominal absence of  $CO_2/HCO_3^-$  in mice, just as we found previously in rats (17),  $H^+$  pumps and/or other extruders could account for a larger share of acid extrusion than we had anticipated. Indeed, Fig-

ures 5 and 6 demonstrate that the Na-independent or HOE 694-insensitive component of acid extrusion is almost as large as the NHE mechanisms. This analysis would also indicate that there are substantial differences in acid-extrusion mechanisms in neurons between rats and mice.

*Reduction of acid extrusion in mutant neurons in the presence of  $\text{HCO}_3^-$ .* With  $\text{CO}_2/\text{HCO}_3^-$  solutions, both WT and mutant neurons increased acid flux rate, indicating that  $\text{HCO}_3^-$ -dependent mechanisms are operative in both types of neurons. Surprising, however, is the fact that (a) the WT neurons had a much larger total flux rate in  $\text{HCO}_3^-$  solutions than did G1 mutant neurons; and (b) the magnitude of the difference in  $\text{H}^+$  flux between mutant and WT neurons was larger in  $\text{HCO}_3^-$  solutions than in the absence of  $\text{HCO}_3^-$  (Figure 4c). We believe that there are 2 potential explanations for this finding. First, it is possible that  $\text{CO}_2/\text{HCO}_3^-$  enhance in the WT neurons (by an unknown mechanism) the activity of NHE1 or other  $\text{H}^+$  extrusion mechanisms (such as  $\text{H}^+$  pump) that may not be activated in mutant neurons and hence exaggerate the difference between mutant and WT neurons. For example, in rat sympathetic neurons, addition of  $\text{HCO}_3^-$  was found to accelerate the  $\text{pH}_i$  recovery from acid load, and this acceleration was unaffected by SITS, suggesting that acid extrusion was mediated by NHE or  $\text{H}^+$  pump (10). Similar results have been reported in rat brain synaptosomes, leech glial cells, and smooth muscles, as well (4, 28, 29). Second, it is possible that the presence or expression of NHE, and in particular NHE1, is important for the full expression (at the transcriptional or translational levels) or proper function of other membrane proteins. We do not know of other exchangers whose expression affect the function of other proteins, but the cystic fibrosis transmembrane regulator (CFTR) has been known to be important for the expression and proper functioning of other membrane channels, such as sodium channels (30) and the outward-rectifier chloride channel (31, 32). Although we do not currently have direct proof for either idea, we believe that, based on previous literature, either is a distinct possibility. However, 2 observations provide support for the second possibility: (a) part of  $\text{HCO}_3^-$ -dependent mechanisms is blockable in the WT mice, but is insensitive to DIDS in the mutant; and (b) the buffering power is lower in the mutant mice, suggesting that the absence of NHE1 plays a role in regulating or expressing other proteins. It is interesting to note in this regard that, as Figure 4d shows, there are at least 2  $\text{HCO}_3^-$ -dependent mechanisms that are present in the WT, but only 1 in the mutant. As expected, the WT has both a DIDS-sensitive and a DIDS-insensitive component; the mutant seems to have lost the sensitive component and has only part of the DIDS-insensitive component. Indeed, as Figure 4d shows, there was a statistically significant difference between the DIDS-insensitive component in the WT and that of the mutant. Of interest is that G2 neurons also have a lower  $\text{HCO}_3^-$ -dependent recovery rate from acid load. Although the

relative number of neurons belonging to this group is small, precluding the detailed study of these neurons in all aspects, it would not be surprising if the  $\text{HCO}_3^-$ -dependent flux in these G2 cells is downregulated, because the recovery rate from an acid load in these G2 neurons in HEPES is even worse than that in G1 cells.

One reason for using CA1 neurons is that the majority of the neurons in that layer are pyramid shaped and form a relatively homogeneous group of cells, although GABAergic interneurons are also scattered in that layer of cells. It was interesting, therefore, that we found a small proportion of neurons (G2) that was very different from the majority of neurons (G1) in the mutant mice. It is possible that these may belong to a separate group of neurons functionally and structurally within that layer of cells. However, we do not believe so because we always studied pyramid-shaped neurons, and it is unlikely that they would be related to interneurons because these latter cells are much smaller. Whether these cells belong to the end of the spectrum (virtually no recovery from acid load even after 10–20 minutes) of the same group of pyramid-shaped neurons is not known. Another important issue that can be raised is whether there are differences between null and WT neurons in terms of their surface/volume ratio. Whereas differences cannot be totally ruled out, our preliminary observation on surface area (data not shown), as reflected by membrane capacitance, are not impressive because null neurons have a larger surface area by only 5–10%. Hence, the downregulation in flux rate in the null neurons, whether in HEPES or in  $\text{CO}_2/\text{HCO}_3^-$ , cannot be explained by differences in size between null and WT neurons.

Although the NHE1 mutation alters markedly  $\text{pH}_i$  regulation in neurons, it is not clear how such differences between WT and mutant neurons lead to the pathophysiology and clinical phenotype seen in these mice, namely ataxia and seizure disorder. At least 2 observations from this work have implications on this issue. First, although mutant neurons have lower steady-state  $\text{pH}_i$  than WT neurons in the absence of  $\text{HCO}_3^-$ , they do not have lower steady-state  $\text{pH}_i$  in physiological solutions. Hence, it is likely that the rate at which neurons respond to an acid challenge, rather than the steady-state  $\text{pH}_i$ , becomes very critical in the overall function of neurons, especially in those that are metabolically active and need to extrude acid at a fast rate. Clearly, an intermittently lower  $\text{pH}_i$  in cells that cannot recover quickly may induce profound changes in neuronal excitability in mutant mice lacking NHE1. From this point of view, it is important to note that these mice do not show a clear neurological phenotype before the age of 3–4 weeks. Whether this is the effect of repeated, intermittent, and chronic pH swings in early life is not clear. It is possible, on the other hand, that the phenotype starts developing when the expression of NHE1 is supposed to occur and reach adult levels. We have shown recently, in fact, that NHE1 expression in the CNS occurs postnatally, mostly after the first week of life (33).



## Acknowledgments

We thank Gregory A. Cox and Wayne Frankel (The Jackson Laboratory) for providing the heterozygous parent mice; Walter Boron and Mark O. Bevensee for their helpful discussions; Steven Brooks for technical assistance; and Hang-J. Lang for his generous gift of HOE 694. This work was supported by National Institute of Health grants P01-NICHD 32573 and NINDS 35918 (to G.G. Haddad).

1. Busa, W.B., and Nuccitelli, R. 1984. Metabolic regulation via intracellular pH. *Am. J. Physiol.* **246**:R409–R438.
2. Chesler, M. 1990. The regulation and modulation of pH in the nervous system. *Prog. Neurobiol.* **34**:401–427.
3. Moody, W., Jr. 1984. Effects of intracellular H<sup>+</sup> on the electrical properties of excitable cells. *Annu. Rev. Neurosci.* **7**:257–278.
4. Nachshen, D.A., and Drapeau, P. 1988. The regulation of cytosolic pH in isolated presynaptic nerve terminals from rat brain. *J. Gen. Physiol.* **91**:289–303.
5. Raley-Susman, K.M., Cragoe, E.J., Jr., Sapolsky, R.M., and Kopito, R.R. 1991. Regulation of intracellular pH in cultured hippocampal neurons by an amiloride-insensitive Na<sup>+</sup>/H<sup>+</sup> exchanger. *J. Biol. Chem.* **266**:2739–2745.
6. Raley-Susman, K.M., Sapolsky, R.M., and Kopito, R.R. 1993. Cl<sup>-</sup>/HCO<sub>3</sub><sup>-</sup> exchange function differs in adult and fetal rat hippocampal neurons. *Brain Res.* **614**:308–314.
7. Bevensee, M.O., Weed, R.A., and Boron, W.F. 1997. Intracellular pH regulation in cultured astrocytes from rat hippocampus. I. Role of HCO<sub>3</sub><sup>-</sup>. *J. Gen. Physiol.* **110**:453–465.
8. Bevensee, M.O., Weed, R.A., and Boron, W.F. 1997. Intracellular pH regulation in cultured astrocytes from rat hippocampus. II. Electrogenic Na<sup>+</sup>/HCO<sub>3</sub><sup>-</sup> cotransport. *J. Gen. Physiol.* **110**:467–483.
9. Gaillard, S., and Dupont, J.L. 1990. Ionic control of intracellular pH in rat cerebellar Purkinje cells maintained in culture. *J. Physiol.* **425**:71–83.
10. Tolkovsky, A.M., and Richards, C.D. 1987. Na<sup>+</sup>/H<sup>+</sup> exchange is the major mechanism of pH regulation in cultured sympathetic neurons: measurements in single cell bodies and neurites using a fluorescent pH indicator. *Neuroscience*. **22**:1093–1102.
11. Richards, C.D., and Tolkovsky, A.M. 1986. The regulation of intracellular pH in rat superior cervical ganglion cells grown on tissue culture. *J. Physiol.* **376**:38P. (Abstr.)
12. Pockock, G., and Richards, C.D. 1989. Hydrogen ion regulation in rat cerebellar granule cells maintained in tissue culture. *J. Physiol.* **412**:68P. (Abstr.)
13. Siesjö, B.K., et al. 1993. Acidosis-related brain damage. *Prog. Brain Res.* **96**:23–48.
14. Ma, E., and Haddad, G.G. 1997. Expression and localization of Na<sup>+</sup>/H<sup>+</sup> exchangers in rat central nervous system. *Neuroscience*. **79**:591–603.
15. Attaphitaya, S., Park, K., and Melvin, J.E. 1999. Molecular cloning and functional expression of a rat Na<sup>+</sup>/H<sup>+</sup> exchanger (NHE5) highly expressed in brain. *J. Biol. Chem.* **274**:4383–4388.
16. Schwiening, C.J., and Boron, W.F. 1994. Regulation of intracellular pH in pyramidal neurons from the rat hippocampus by Na<sup>+</sup>-dependent Cl<sup>-</sup>/HCO<sub>3</sub><sup>-</sup> exchange. *J. Physiol.* **475**:59–67.
17. Bevensee, M.O., Cummins, T.R., Haddad, G.G., Boron, W.F., and Boyarsky, G. 1996. pH regulation in single CA1 neurons acutely isolated from the hippocampi of immature and mature rats. *J. Physiol.* **494**:315–328.
18. Friedman, J.E., and Haddad, G.G. 1993. Major differences in Ca<sub>v</sub><sup>2+</sup> response to anoxia between neonatal and adult rat CA1 neurons: role of Ca<sub>v</sub><sup>2+</sup> and Na<sub>v</sub><sup>2+</sup>. *J. Neurosci.* **13**:63–72.
19. Cox, G.A., et al. 1997. Sodium/hydrogen exchanger gene defect in slow-wave epilepsy mutant mice. *Cell*. **91**:139–148.
20. Thomas, J.A., Buchsbaum, R.N., Zimniak, A., and Racker, E. 1979. Intracellular pH measurements in Ehrlich ascites tumor cells utilizing spectroscopic probes generated in situ. *Biochemistry*. **18**:2210–2218.
21. Boyarsky, G., Ganz, M.B., Sterzel, R.B., and Boron, W.F. 1988. pH regulation in single glomerular mesangial cells. I. Acid extrusion in absence and presence of HCO<sub>3</sub><sup>-</sup>. *Am. J. Physiol.* **255**:C844–C856.
22. Roos, A., and Boron, W.F. 1981. Intracellular pH. *Physiol. Rev.* **61**:389–392.
23. Bevensee, M.O., Schwiening, C.J., and Boron, W.F. 1995. Use of BCECF and propidium iodide to assess membrane integrity of acutely isolated CA1 neurons from rat hippocampus. *J. Neurosci. Med.* **58**:61–75.
24. Boron, W.F., and De Weer, P. 1976. Intracellular pH transients in squid giant axons caused by CO<sub>2</sub>, NH<sub>3</sub>, and metabolic inhibitors. *J. Gen. Physiol.* **67**:91–112.
25. Anderie, I., Blum, R., Haase, W., Grinstein, S., and Thevenod, F. 1998. Expression of NHE1 and NHE4 in rat pancreatic zymogen granule membranes. *Biochem. Biophys. Res. Commun.* **246**:330–336.
26. Counillon, L., Scholz, W., Lang, H.J., and Pouyssegur, J. 1993. Pharmacological characterization of stably transfected Na<sup>+</sup>/H<sup>+</sup> antiporter isoforms using amiloride analogs and a new inhibitor exhibiting anti-ischemic properties. *Mol. Pharmacol.* **44**:1041–1045.
27. Scholz, W., et al. 1993. Hoe 694, a new Na<sup>+</sup>/H<sup>+</sup> exchange inhibitor and its effects in cardiac ischaemia. *Br. J. Pharmacol.* **109**:562–568.
28. Deitmer, J.W., and Schlue, W.R. 1985. Measurement of intracellular pH in identified leech glial cells using double-barrelled micro-electrodes. *J. Physiol. (Lond.)* **371**:154P. (Abstr.)
29. Claire Aickin, C. 1984. Direct measurement of intracellular pH and buffering power in smooth muscle cells of guinea-pig vas deferens. *J. Physiol.* **349**:571–585.
30. Stutts, M.J., et al. 1995. CFTR as a cAMP-dependent regulator of sodium channels. *Science*. **269**:847–850.
31. Egan, M., et al. 1992. Defective regulation of outwardly rectifying Cl<sup>-</sup> channels by protein kinase A corrected by insertion of CFTR. *Nature*. **358**:581–584.
32. Hwang, T.C., et al. 1989. Cl<sup>-</sup> channels in CF: lack of activation by protein kinase C and cAMP-dependent protein kinase. *Science*. **244**:1351–1353.
33. Douglas, R.M., Xia, Y., Biemesderfer, D., and Haddad, G.G. 1997. Modulation of the sodium hydrogen exchanger: effect of development and hypoxic stress. *Soc. Neurosci. Abstr.* **23**:6119. (Abstr.)